journal

J. Am. Ceram. Soc., **81** [12] 3150–56 (1998)

Dependence of Oxidation Modes on Zirconia Content in Silicon Carbide/Zirconia/Mullite Composites

Cheng-Yuan Tsai and Chien-Cheng Lin*,†

Department of Materials Science and Engineering, National Chiao Tung University, Hsinchu 300, Taiwan

Two basic oxidation modes of silicon carbide/zirconia/mullite (SiC/ZrO_2/mullite) composites were defined based on the plotted curve of the gradient of the silica (SiO_2) layer thickness (formed on individual SiC particles) versus depth. Mode I, where oxygen diffusivity was much slower in the matrix than in the SiO_2 layer, exhibited a relatively large gradient and limited oxidation depth. Mode II, where oxygen diffusivity was much faster in the matrix than in the SiO_2 layer, displayed a relatively small gradient and an extensive oxidation depth. When the volume fraction of ZrO_2 was below a threshold limit, the composites exhibited Mode I behavior; otherwise, Mode II behavior was observed. For composites with a ZrO_2 content above the threshold limit, the formation of zircon ($ZrSiO_4$), as a result of the reaction between ZrO_2 and the oxidation product (i.e., SiO_2), might change the oxidation behavior from Mode II to Mode I.

I. Introduction

MULLITE is an excellent matrix material for ceramic-matrix composites (CMCs), because of features such as its high-temperature properties, low oxygen permeability, and chemical inertness. However, this material is limited primarily by its extremely low fracture toughness.[1–3] Therefore, to enhance its fracture toughness, mullite-based composites must be developed. In general, ceramics that incorporate silicon carbide (SiC) whiskers and/or partially stabilized zirconia (PSZ) are tougher than conventional monolithic ceramics.[4–8] However, at high temperatures, the instability and deterioration of SiC-containing CMCs via oxidation are of particular concern.[9–12]

Many investigators[13–21] have examined the oxidation behavior of SiC-reinforced mullite and zirconia (ZrO_2)/mullite matrix composites at elevated temperatures. However, the researchers of most related works did not realize that the composites could demonstrate a very different oxidation behavior, because of the variation of compositions. Recently, Lin and co-workers[22,23] elucidated the oxidation behavior of SiC-reinforced mullite matrix and ZrO_2/mullite matrix composites after exposure to air at 1000°–1350°C. According to their results, two basic oxidation modes were proposed on the basis of the relationship between the oxygen diffusivity in the matrix and in the oxide layer. Mode I was defined as the case where oxygen diffused through the matrix so slowly that oxygen could still react with incompletely oxidized SiC whiskers before it diffused further into the matrix, resulting in a small oxidation depth and a clear boundary between the substrate and the oxidized outer region. Mode II was defined as the case where oxygen diffused through the matrix so rapidly that oxygen could penetrate deeply into the matrix before SiC whiskers in the outer region were completely oxidized, leaving behind a long range of partially oxidized SiC whiskers. In addition, a mixed mode (i.e., pure or modified Mode II followed by Mode I, designated as Mode ''II+I'') might occur because of subsequent chemical reaction between the matrix and the oxidation product. Such a reaction could dramatically change the oxygen diffusivity through the matrix during long-term exposure at high temperatures.

A previous study presented a theoretical model to rationalize the oxidation-mode concepts. Zangvil *et al.*[24] claimed that the silica (SiO_2) layer thickness around each oxidizing SiC platelet was not only a function of the oxygen diffusivity in the matrix and in the individual SiO_2 layer, but also of the depth of each SiC platelet in the matrix. According to their results, the oxidation behavior of SiC-platelet-reinforced mullite–40 vol% ZrO_2 composites was categorized as Mode II, which contained a large range of partially oxidized SiC platelets.

Tsai *et al.*[25] examined how the ZrO_2 content of SiC/ZrO_2/mullite composites influenced the oxidation mechanism and morphology. According to their results, the oxidation rate dramatically increased as the ZrO_2 content exceeded a certain threshold volume fraction, whereas below this limit, the oxidation rate remained fairly low. At 1200°C, the formation of zircon ($ZrSiO_4$), because of reaction between the matrix and the oxidation product, probably caused a sharp decrease in the oxidation rate, depending on the extent of ZrO_2 consumption. In addition, the composites that contained more ZrO_2 than the threshold value exhibited a large oxidation depth and vice versa. However, to date, the oxidation modes of the composites with various ZrO_2 contents have not been systematically investigated. In this study, we have closely examined how ZrO_2 content influences the oxidation modes by plotting the curves of the thickness of the oxide layer formed on each SiC particle with respect to its depth below the surface. Also discussed herein is the effect of the formation of $ZrSiO_4$ on the oxidation modes.

II. Experimental Procedure

Composites of silicon carbide particles, zirconia, and mullite (SiC_p/ZrO_2/mullite), all of which contained 30 vol% SiC particulate and were fabricated via the hot pressing technique, were isothermally exposed to air at 1000° and 1200°C. Each of the specimens was placed in a mullite crucible and then loaded in a box furnace (Model 51333, Lindberg, Watertown, WI) as the exposure temperature was reached. Details of the oxidation test can be found elsewhere.[25]

Table I lists the composition, hot-pressing conditions, density, and X-ray diffractometry (XRD) phases of each composite. For convenience, the ''zirconia+mullite'' in each SiC_p/ZrO_2/mullite composite is called the ''matrix,'' although the matrix itself is a composite. The zirconia+mullite matrix content is 70 vol% in each composite, whereas the ZrO_2 content is stated in terms of the matrix itself rather than the entire composite.

D. P. Butt—contributing editor

Manuscript No. 190925. Received December 15, 1997; approved March 10, 1998.
Supported by the National Science Council, Taiwan, under Grant No. NSC83-0405-E-009-006.

*Member, American Ceramic Society.
†Author to whom correspondence should be addressed.

Table I. Designation, Compositions, Hot-Pressed Conditions, Densities, and XRD Phases of Composites

Composite	Composition†	Hot-pressing conditions‡	Relative density (%)	XRD phases present§
MZY15/SiC	(Mullite + 15 vol% 3Y-PSZ) + 30 vol% SiC	1600°C/45 min	99.1	M, α-SiC, t-Z, m-Z
MZY20/SiC	(Mullite + 20 vol% 3Y-PSZ) + 30 vol% SiC	1600°C/45 min	99.0	M, α-SiC, t-Z, m-Z
MZY25/SiC	(Mullite + 25 vol% 3Y-PSZ) + 30 vol% SiC	1600°C/45 min	98.3	M, α-SiC, t-Z, m-Z
MZY30/SiC	(Mullite + 30 vol% 3Y-PSZ) + 30 vol% SiC	1600°C/45 min	98.5	M, α-SiC, t-Z, m-Z
MZY50/SiC	(Mullite + 50 vol% 3Y-PSZ) + 30 vol% SiC	1600°C/45 min	98.3	M, α-SiC, t-Z, m-Z
MZY80/SiC	(Mullite + 80 vol% 3Y-PSZ) + 30 vol% SiC	1600°C/45 min	98.0	M, α-SiC, t-Z, m-Z
MZY100/SiC	3Y-PSZ + 30 vol% SiC	1600°C/45 min	99.9	α-SiC, t-Z, m-Z

†The matrix content (in parentheses) is 70 vol% for each composite; the balance is SiC_p. The ZrO_2 content is stated in terms of the matrix itself; i.e., the amount of Y-PSZ(vol%) = [(volume of Y-PSZ)/(volume of mullite + volume of Y-PSZ)] × 100. ‡Hot pressing was conducted under a pressure of 30 MPa in a 1 atm argon atmosphere. §''M'' is mullite, ''t-Z'' is tetragonal zirconia (t-ZrO_2), and ''m-Z'' is monoclinic zirconia (m-ZrO_2).

The major phases on the exposed samples were identified by using XRD (Model MXP18, Mac Science, Tokyo, Japan). The oxide layer thicknesses of individual SiC particles at various depths were measured using scanning electron microscopy (SEM) (Model S-2500, Hitachi, Tokyo, Japan) and transmission electron microscopy (TEM) (Model 2000FX, JEOL, Tokyo, Japan). Prior to doing so, the cross-sectional samples were prepared as follows. Each oxidized sample was cut into two halves in a direction perpendicular to the exposed surface, followed by ultrasonically cleaning in acetone. Two halves of the oxidized surfaces were glued together facing each other by using epoxy (G-1 epoxy, Gatan, Pleasanton, CA), while applying a proper force, and heated to 100°C for 5 min. Slices ~300 μm thick were cut perpendicular to the surface and then ground on a precision polishing machine (Model Minimet® 1000, Buehler Ltd., Lake Bluff, IL) with 0.5 μm diamond paste. The cross-sectional slab was thinned to 10–20 μm (finished preparation of SEM samples) and finally argon-ion-milled at 5 kV and 1 mA. To avoid charging, all the SEM and TEM samples were coated with a thin layer of carbon. The oxide layer thicknesses of SiC particles at different depths were then examined via SEM and/or TEM; both were equipped for energy-dispersive X-ray spectrometry (EDS). The average SiO_2 layer thickness was taken from SEM and/or TEM observations on several SiC particles at the same depth. However, the small SiO_2 thicknesses for slightly oxidized SiC particles in the inner region had to be determined via TEM, because of the limited resolution of the SEM equipment.

III. Results and Discussion

(1) Microstructural Observations

Table I lists the densities of as-hot-pressed samples. All the densities were >98% of their corresponding theoretical densities. Meanwhile, no additional phases were observed, except those which were inherited from the raw materials.

Figure 1 is a TEM micrograph of the as-hot-pressed MZY15/SiC composite; this figure reveals a typically dense microstructure. SiC particles have an angular shape, whereas the mullite particles seem to have an almost-rectangular shape. Two types of ZrO_2 were observed: one was small and spherical (tetragonal zirconia, t-ZrO_2) and was embedded in the mullite grain, and the other was angular and located along grain boundaries (coexisting as t-ZrO_2 and monoclinic zirconia (m-ZrO_2)). This observation is consistent with the results from a previous study.[26]

Figures 2 and 3 depict distinct microstructures viewed from the cross-sectional direction perpendicular to the surfaces of two exposed samples. Figure 2 presents an SEM micrograph of the MZY25/SiC composite after exposure at 1200°C for 500 h. The gray lumpy phase encircled by a dark layer is SiC, the bright phase is ZrO_2, and the gray matrix is mullite; the outer surface is on the left portion of the micrograph. SiC particles in the outer region began to oxidize and, then, each of them was surrounded by a layer of oxidation product, which was identified via EDS as SiO_2. SiC particles were partially oxidized all the way from the surface to a depth of >450 μm, which is beyond the field of view. This observation indicates that the MZY25/SiC composite had an extensive oxidation zone after exposure at 1200°C for 500 h. Figure 2 also shows how the thickness of the SiO_2 layer varied with respect to the depth of the corresponding SiC particles. The SiO_2 layer in the outer region, from the surface to a depth of ~120 μm, was much thicker than that in the inner region. Figure 3 depicts two oxidation microstructures of the MZY15/SiC composite after exposure at 1200°C for 500 h. Figure 3(a) illustrates an SEM cross-sectional view, indicating a more extremely limited oxidation depth than that in Fig. 2. The SiO_2 layer thickness in the outer region could be easily measured through SEM observations. However, this was not the case for the extremely thin SiO_2 layer of the individual SiC particle in the inner region, because of the resolution limitation of SEM. Figure 3(b) presents a TEM micrograph of the MZY15/SiC composite, revealing an extremely thin SiO_2 layer (~30 nm thick) around a SiC particle at a depth of 38 μm.

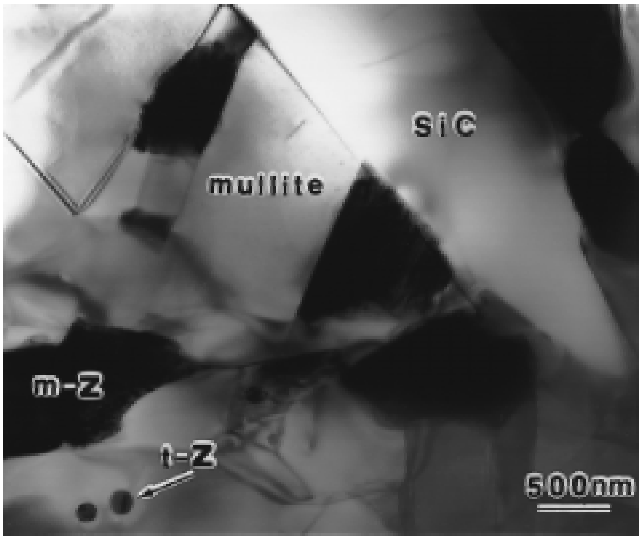

Fig. 1. TEM micrograph showing the dense microstructure of the as-hot-pressed MZY15/SiC composite (''m-Z'' = m-ZrO_2 and ''t-Z'' = t-ZrO_2).

(2) Silica Layer Thickness versus Depth Curves

(A) Oxidation at 1000°C: Figure 4 illustrates the SiO_2 layer thicknesses at different depths for various composites after exposure at 1000°C for 500 h in air. SiC particles at the outer surfaces were not completely oxidized after long-term exposure, because the average size of a SiC particle was assumed to be ~7 μm and the thickest SiO_2 layer in the MZY100/SiC composite was ~1 μm. The curve for the MZY20/SiC composite in Fig. 4 had a relatively steep slope (ranging from -8×10^{-3} to -30×10^{-3}), with a limited oxidation depth of ~40 μm. In contrast, the curves for the MZY30/SiC, MZY50/SiC, and MZY100/SiC composites had much shallower slopes

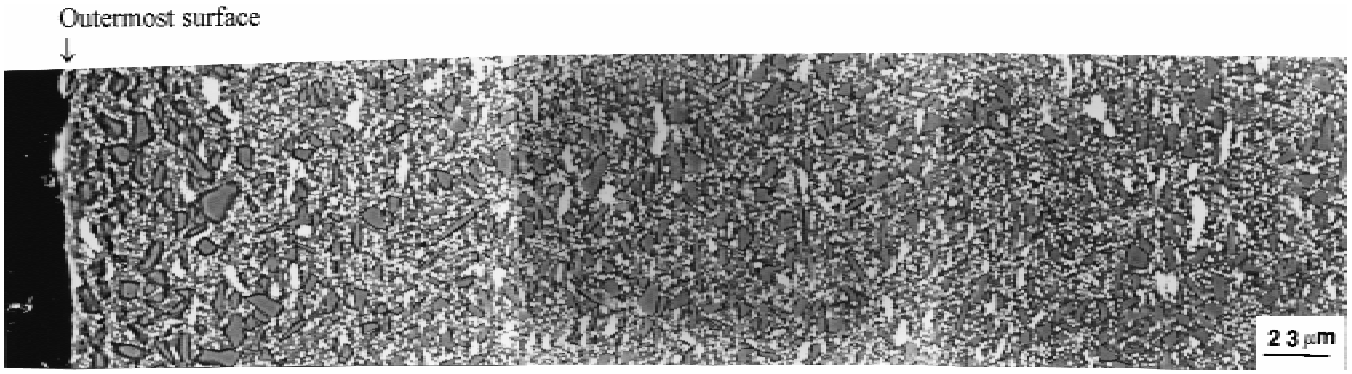

Fig. 2. SEM cross-sectional view of the MZY25/SiC composite after exposure at 1200°C for 500 h, revealing a large oxidized zone as well as the variation of the SiO_2 layer thickness with depth. SiC particles were partially oxidized all the way from the surface to a depth of >450 μm, which is beyond the field of view.

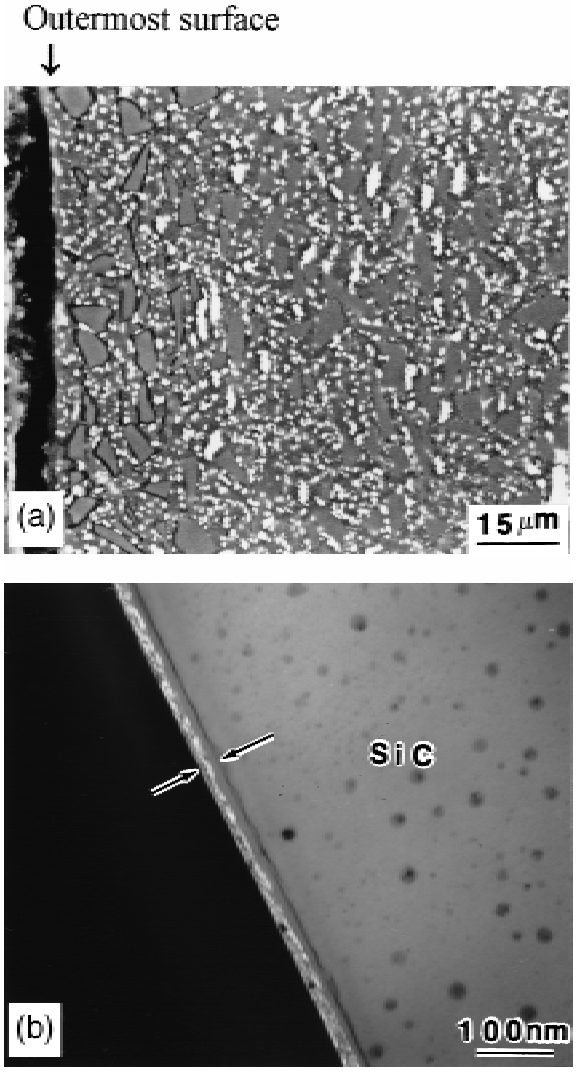

Fig. 3. Microstructures of the MZY15/SiC composite after exposure at 1200°C for 500 h ((a) SEM cross-sectional view indicating a very limited oxidized zone, compared to that shown in Fig. 2, and (b) TEM micrograph showing a thin SiO_2 layer ~300 Å thick around a SiC particle at the depth of 38 μm).

(ranging from -0.6×10^{-3} to -4×10^{-3}) with much greater oxidation depths than that of the MZY20/SiC composite. The difference between the MZY20/SiC and MZY30/SiC composites (or composites that contain >30 vol% ZrO_2) implies a dramatic transition in oxidation behavior with changes in ZrO_2 content. The ZrO_2 content where this transition occurred is the so-called ''percolation threshold,'' which was ~20 vol% ZrO_2 based on the weight-gain data in the previous study.[25] In addition to the measurements of the SiO_2 layer thickness, Lin and co-workers[22,23] characterized the oxidation behavior of the exposed composites, based on the oxidation morphologies related to whether SiC particles were completely oxidized within the outer region of the composite. However, the oxidation mode in this study was determined based on the plotted curve of SiO_2 layer thickness versus depth. Mode I was characterized by a small oxidation depth and a comparatively large gradient of the curve of SiO_2 layer thickness versus depth. Meanwhile, Mode II was characterized by a large oxidation depth and a relatively small gradient. Each of the composites that have a ZrO_2 content that is greater than the percolation threshold exhibited a similar tendency, as characterized by a small gradient and a large oxidation depth. The slope for Mode II was approximately one order of magnitude smaller than that for Mode I. In addition, the SiO_2 layer thicknesses of those composites at the corresponding depths increased as the ZrO_2 content increased; the largest oxidation rate was observed in the MZY100/SiC composite, followed by that of the MZY50/SiC composite. The severe oxidation of the MZY100/SiC composite corresponded to the higher ZrO_2 content in the MZY100/SiC composite than in other composites, which leads to faster oxygen transport routes via ZrO_2.

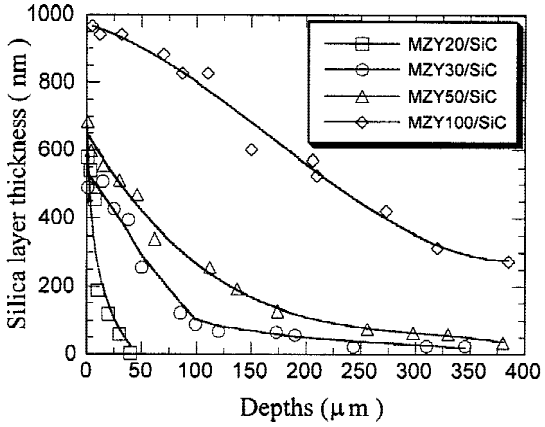

Fig. 4. SiO_2 layer thicknesses at various depths after exposure at 1000°C for 500 h.

Figure 5(a) displays the curves of SiO_2 layer thickness versus depth of the MZY20/SiC composite for various times after exposure at 1000°C. Each curve exhibits a steep slope. The SiO_2 layer thickness at the outermost surface increases as the time increases but then rapidly decreases to zero at depths of

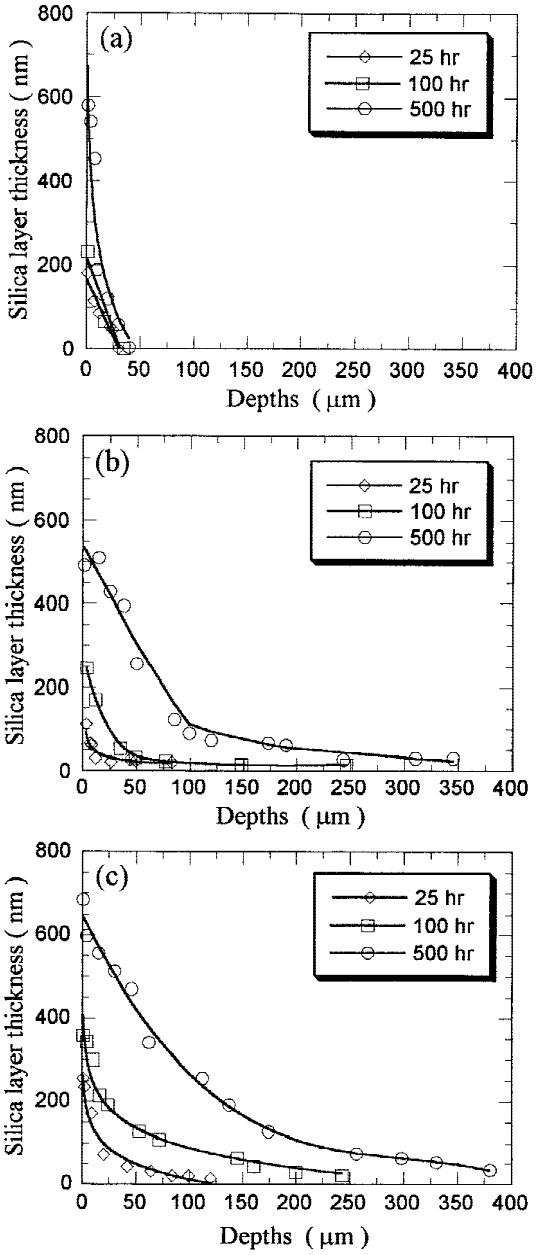

Fig. 5. Curves of SiO_2 layer thickness versus depth at various intervals ((a) MZY20/SiC, (b) MZY30/SiC, and (c) MZY50/SiC composites, all after exposure at 1000°C).

~30–40 μm. With a large slope and a limited oxidation depth, the oxidation behavior of the MZY20/SiC composite at 1000°C was categorized as Mode I. Figure 5(b) indicates that the MZY30/SiC composite, for various times, had a similar tendency to have a small slope and a large oxidation depth. Evidently, oxygen could more easily and deeply diffuse in the MZY30/SiC composite than in the MZY20/SiC composite, which implied that oxygen diffusivity in the matrix of the MZY30/SiC composite was markedly larger than that in the matrix of the MZY20/SiC composite, as a consequence of the rapid transport paths via ZrO_2 in the MZY30/SiC composite. Figure 5(c) illustrates the SiO_2 layer thickness of the MZY50/SiC composite at different depths for various intervals. Those results are analogous to the corresponding case of the MZY30/SiC composite; both show an extensive oxidation depth. With a small slope and a large oxidation depth, the oxidation modes for both the MZY30/SiC and MZY50/SiC composites at 1000°C were thus classified as Mode II.

(B) Oxidation at 1200°C: Figure 6 depicts the curves of the SiO_2 layer thickness versus depth for various composites after exposure at 1200°C for 25 h. According to this figure, several composites exhibited very different behavior during oxidation. The characteristic of a steep slope (approximately -13×10^{-3}) with a small oxidation depth was observed in the MZY15/SiC composite, compared with much-smaller slopes (ranging from -0.6×10^{-3} to -6×10^{-3}) for the MZY50/SiC and MZY100/SiC composites. This observation is analogous to that for the MZY20/SiC composite at 1000°C; thus, the oxidation behavior of the MZY15/SiC composite was Mode I. However, the oxidation behavior markedly differed among the MZY25/SiC, MZY50/SiC, and MZY100/SiC composites. For the MZY25/SiC composite after exposure at 1200°C for 25 h, the curve could be divided into two regions, based on very different slopes: the outer region had a larger negative slope (approximately -26×10^{-3}), whereas the inner region had a smaller negative slope (approximately -0.4×10^{-3}) with slightly oxidized SiC. The fact that the behavior of the MZY25/SiC composite at 1200°C for 25 h encompassed two distinctive regions implies that the oxidation mode changed during exposure, because of the formation of $ZrSiO_4$, as discussed later. Thus, the oxidation mode of the MZY25/SiC composite at 1200°C for 25 h was categorized as Mode II+I or a mixed mode, as defined previously.[22,23] Interestingly, after exposure at 1200°C for 25 h, the MZY50/SiC composite rather than the MZY100/SiC composite had the thickest SiO_2 layer at corresponding depths. This outcome differed from exposures at 1000°C for 500 h. This observation was also attributed to the presence of $ZrSiO_4$, which resulted from the reaction between ZrO_2 and SiO_2 at 1200°C. More ZrO_2 particles accounted for a larger quantity and an earlier formation of $ZrSiO_4$ in the composites. Without any evident change in slope, but with a larger oxidation depth, the oxidation mode of the MZY50/SiC composite at 1200°C for 25 h was classified as Mode II; the oxidation mode for the MZY100/SiC composite was also classified as Mode II.

Figure 7(a) displays the curves of SiO_2 layer thickness versus depth for the MZY15/SiC composite at various intervals. Similar to the MZY20/SiC composite at 1000°C, the MZY15/SiC composite after exposure at 1200°C exhibited Mode I oxidation. Figure 7(b) presents the curves of the SiO_2 layer thickness versus depth for the MZY25/SiC composite at different intervals. For exposure after 9 h, the oxidation behavior should be categorized as Mode II, because the composite has a much smaller gradient and a much larger oxidation depth than that of the MZY15/SiC composite at 1200°C for 500 h. However, after exposure for 25 h, the dashed curve, purposely used as an indication of the change in oxidation mode, denoted two distinct slopes that contained a steep slope in the outer region, followed by a dramatic decrease in slope with extensive slightly oxidized SiC in the inner region. As mentioned previ-

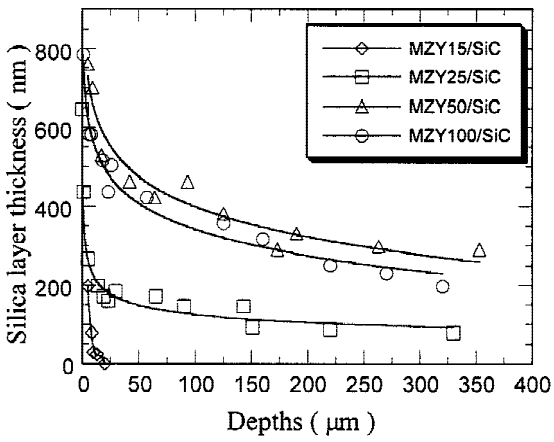

Fig. 6. SiO_2 layer thicknesses at various depths, all after exposure at 1200°C for 25 h.

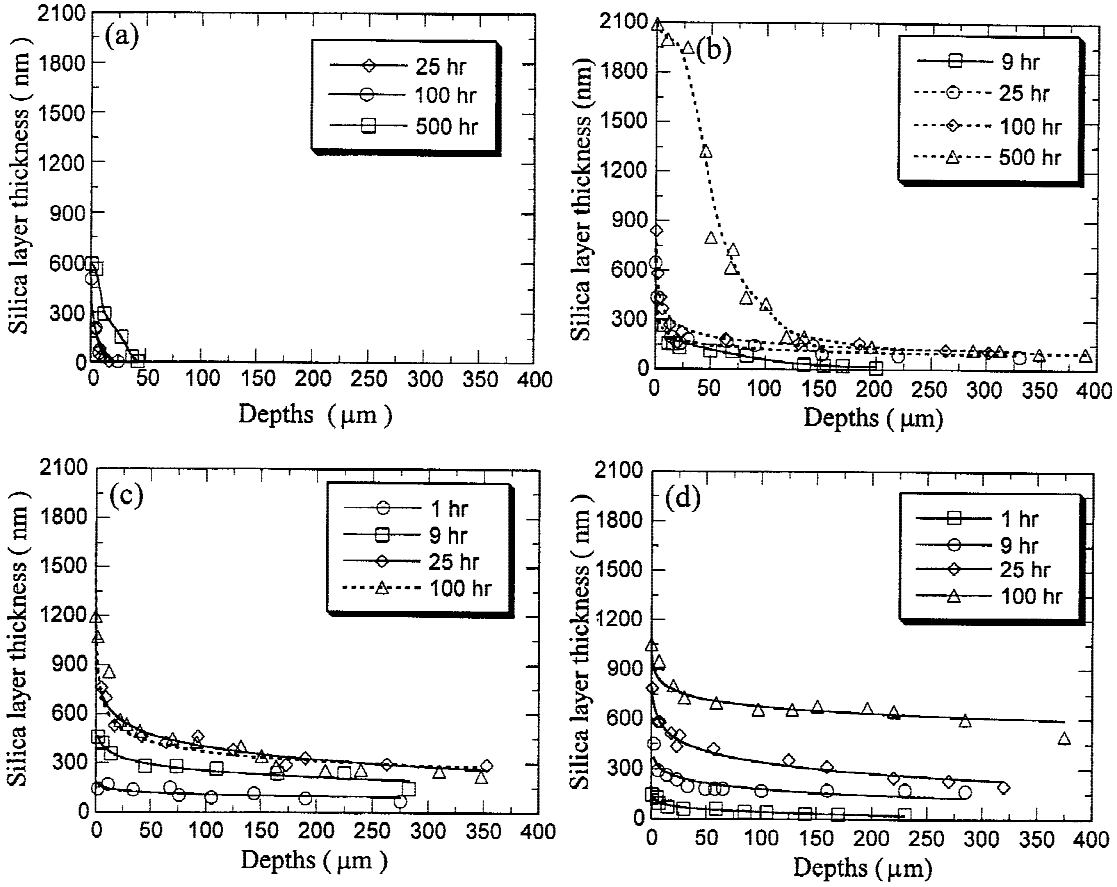

Fig. 7. Curves of SiO_2 layer thickness versus depth at various intervals ((a) MZY15/SiC, (b) MZY25/SiC, (c) MZY50/SiC, and MZY100/SiC composites, all after exposure at 1200°C).

ously, the oxidation mode was the mixed mode (Mode II+I). Similarly, for 100 and 500 h, both curves could again be distinguished by two very different slopes. It is also noted that the SiO_2 layer thickness in the outer region sharply increased as the time increased, whereas the SiO_2 layer thickness in the inner region had a tendency not to differ markedly, even for a sufficiently long time. In other words, the SiO_2 layer in the inner region did not thicken after the oxidation behavior changed from Mode II to Mode I. In contrast, the SiO_2 layer thickness of the inner region for Mode II continued to increase as the time increased, as indicated in Figs. 5(b) and (c).

Figure 8 illustrates XRD spectra of the MZY25/SiC composite at 1200°C; this figure indicates the formation of cristobalite and $ZrSiO_4$. Cristobalite, formed by the devitrification of amorphous silica, was detected after exposure for 9 h; meanwhile, $ZrSiO_4$ (i.e. the reaction product of ZrO_2 and SiO_2) was detected after exposure for 25 h. The amounts of $ZrSiO_4$ and cristobalite both increased as the time increased. This observation suggests that the devitrification of amorphous silica was continuously occurring while the remaining SiO_2 was gradually consumed in the chemical reaction with ZrO_2. The formation of $ZrSiO_4$ could strongly influence the oxidation rate of the MZY25/SiC composite, even if the amount of composite is small. Such an influence was attributed to the fact that the oxygen diffusion rate in $ZrSiO_4$ was much slower than that in ZrO_2.[27] Correspondingly, the rapid diffusion routes via ZrO_2 were disconnected. Thus, for the MZY25/SiC composite, after the ZrO_2 content quickly decreased below the threshold value, its oxidation behavior would change from Mode II to Mode I. As mentioned elsewhere,[23] Mode I prevailed when the oxygen diffusivity was much slower in the matrix than in the SiO_2 layer. The formation of $ZrSiO_4$ would favor the transition from Mode II to Mode I, because it caused a dramatic decrease in the oxygen diffusivity through the matrix. Conversely, Mode II prevailed when the oxygen diffusivity was much faster in the matrix than in the SiO_2 layer.[23] The devitrification of amorphous silica to cristobalite, which causes a decrease in the oxygen diffusivity through the SiO_2 layer,[28] would favor Mode II. However, the fact that the oxidation mode changed from Mode II to Mode I in this study implies that the formation of $ZrSiO_4$ was the controlling factor.

Figure 7(c) depicts the SiO_2 layer thicknesses at various depths for the MZY50/SiC composite at various intervals. According to those results, a similar tendency resulted, with a small gradient and a large oxidation depth for exposure of <25 h. Without any dramatic slope change, their oxidation could be classified as Mode II. However, after exposure for 100 h, the curve could be considered to have two regions with very different slopes, which would be characterized as mixed-mode oxidation. Correspondingly, for the composites that had a ZrO_2 content immediately above the threshold volume fraction, e.g., the MZY25/SiC composite, the oxidation behavior was quite sensitive to the formation of $ZrSiO_4$, which caused a reduction in the ZrO_2 content. The change in oxidation mode occurred when the residual ZrO_2 content was lower than the threshold volume fraction. In contrast, the oxidation behavior of the MZY50/SiC composite should be less susceptible to the presence of $ZrSiO_4$ than that of the MZY25/SiC composite at 1200°C, because the MZY50/SiC composite had a higher ZrO_2 content than did the MZY25/SiC composite. Therefore, the change in oxidation mode should be delayed in the MZY50/SiC composite at 1200°C. In the inner region, the curve for the 100-h exposure fell slightly below that for 25-h exposure, which was attributed to the data scatter and the subsequent curve fitting. Figure 7(d) displays the curves for the MZY100/SiC composite at different intervals; this figure indicates that the oxidation mode did not change and all the oxidation modes were Mode II.

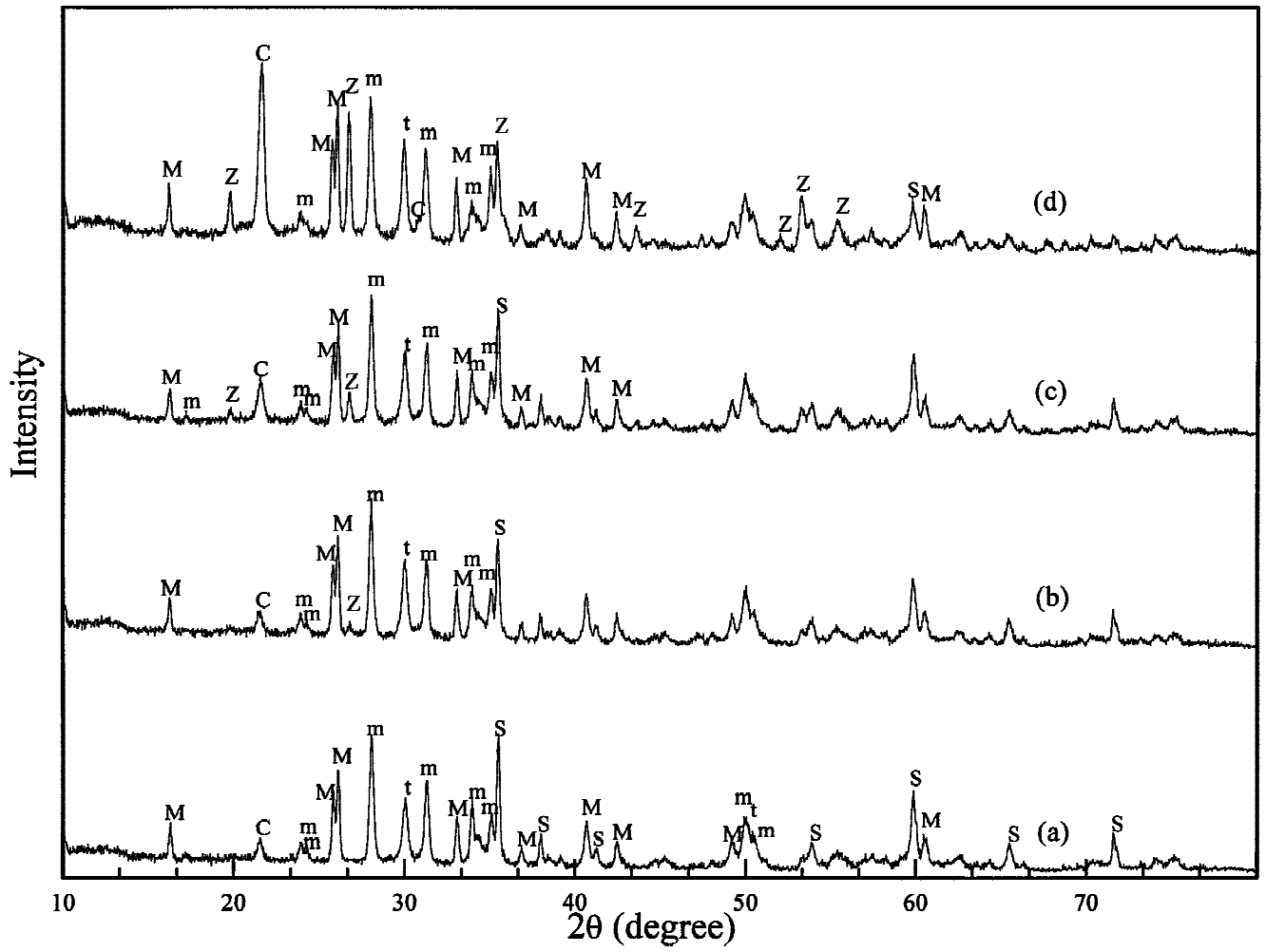

Fig. 8. XRD spectra of the surface of the MZY25/SiC composite after exposure at 1200°C for 9 h (spectrum ''(a)''), 25 h (spectrum ''(b)''), 100 h (spectrum ''(c)''), and 500 h (spectrum ''(d)'') (''M'' is mullite, ''C'' is cristobalite, ''S'' is SiC, ''Z'' is zircon, ''m'' is monoclinic ZrO_2, and ''t'' is tetragonal ZrO_2).

(3) Effect of the Formation of Zircon

The change in oxidation mode after long-term exposure at 1200°C was attributed to the formation of $ZrSiO_4$, which could be expressed as follows:

$$SiC + ZrO_2 + \tfrac{3}{2}O_2 \rightarrow ZrSiO_4 + CO \quad (1)$$

Assuming the densities of ZrO_2 and SiC to be 6.0 and 3.21 g/cm^3, respectively, and the atomic weights of ZrO_2 and SiC to be 123.2 and 40 g/mol, respectively, the percentage of SiC (x) allowed to be oxidized before the volume fraction of the remaining ZrO_2 (z) decreased below the threshold value was calculated by using the following equation:

$$x(\%) = \frac{3.41(z - 0.2)}{2.41} \times 100 \quad (2)$$

This calculation is based on a ZrO_2 threshold value of 20 vol%, as reported in a previous investigation.[25] Table II summarizes the calculated results. The fact that the formation of $ZrSiO_4$ requires solid-state diffusion explains why the calculation merely reflects a lower limiting case. On the other hand, the available SiC (30 vol%), at any depth or region, is assumed to be completely oxidized and then continuously react with ZrO_2 after sufficiently long-term exposure. For composites in this study, up to 71 vol% of ZrO_2, if available, could be consumed from the matrix because of the formation of $ZrSiO_4$. Therefore, the composite did not undergo a change in oxidation mode during long-term exposure when the ZrO_2 content of the as-hot-pressed composite was >91 vol%. Table III lists the amounts of residual ZrO_2 in various composites after sufficiently long-term exposure. This table indicates that, in the MZY100/SiC composite, 29 vol% of ZrO_2 still remained after completely reacting with the available SiO_2. Because the fast-diffusion routes via ZrO_2 continued to operate, the oxidation mode likely remained as Mode II. Conversely, the ZrO_2 contents in the MZY25/SiC and MZY50/SiC composites were reduced below the threshold limit after extremely long-term exposures. As a result, the oxidation mode was modified from Mode II to Mode I, which led to a dramatic decrease in oxi-

Table II. Theoretical Amount of Original SiC Allowed to be Oxidized before the ZrO_2 Content Decreases below the Threshold Value

Composite	Permissible SiC content (%)
MZY15/SiC	
MZY25/SiC	7
MZY30/SiC	14
MZY50/SiC	43
MZY80/SiC	85
MZY100/SiC	113

Table III. Oxidation Modes and Residual ZrO_2 Contents after Sufficiently Long-Term Exposure at 1200°C

Composite	Original ZrO_2 content (vol%)	Oxidation mode prior to zircon formation	Residual ZrO_2 content (vol%) after sufficiently long-term exposure	Oxidation mode after sufficient long-term exposure	Overall oxidation mode
MZY15/SiC	15	Mode I	0	Mode I	Mode I
MZY25/SiC	25	Mode II	0	Mode I	Mode II+I
MZY30/SiC	30	Mode II	0	Mode I	Mode II+I
MZY50/SiC	50	Mode II	0	Mode I	Mode II+I
MZY80/SiC	80	Mode II	9	Mode I	Mode II+I
MZY100/SiC	100	Mode II	29	Mode II	Mode II

dation rate. The oxidation modes at 1200°C for various composites, prior to the formation of $ZrSiO_4$ as well as after sufficiently long-term exposures, are also summarized in Table III.

IV. Conclusions

This study investigated the oxidation behavior of SiC-reinforced ZrO_2/mullite matrix composites by examining the relationship between the SiO_2 layer thickness and the depth of the corresponding SiC particle below the outermost surface. Two basic oxidation modes for the SiC/ZrO_2/mullite composites were defined: (i) Mode I, where the oxygen diffusivity is much slower in the matrix than in the SiO_2 layer, and a relatively large gradient and a limited oxidation depth are exhibited, and (ii) Mode II, where the oxygen diffusivity is much faster in the matrix than in the SiO_2 layer, and a relatively small gradient and an extensive oxidation depth are shown. Oxidation modes of the exposed composites were related to their ZrO_2 content:

(1) Below the threshold limit of ZrO_2 content and without $ZrSiO_4$ formation (e.g., the MZY20/SiC composite after long-term exposures at 1000°C), the oxidation mode exhibited Mode I behavior.

(2) When the ZrO_2 content exceeded the threshold limit and did not form any $ZrSiO_4$ (e.g., the MZY30/SiC, MZY50/SiC, or MZY100/SiC composites at 1000°C), the composites exhibited Mode II behavior.

(3) Below the threshold limit of ZrO_2 content and with $ZrSiO_4$ formation (e.g., the MZY15/SiC composite after long-term exposures at 1200°C), the oxidation mode exhibited Mode I behavior.

(4) Identification of the oxidation mode was more complicated when the ZrO_2 content exceeded the threshold limit and $ZrSiO_4$ formed after relatively long-term exposure at 1200°C. When ZrO_2 content decreased below the threshold limit, because of the replacement of ZrO_2 by $ZrSiO_4$ (such as the case for the MZY25/SiC or MZY50/SiC composites), the oxidation behavior was categorized as mixed mode, consisting of Mode II and subsequent Mode I. If the ZrO_2 content was still higher than the threshold limit after the replacement (such as the case for the MZY100/SiC composite), the oxidation mode was Mode II.

Acknowledgment: The authors would like to thank Professor Avigdor Zangvil of the University of Illinois at Urbana–Champaign (Urbana, IL) for the helpful discussions.

References

[1]S. Kanzaki, H. Tabata, T. Kumazawa, and S. Ohta, ''Sintering and Mechanical Properties of Stoichiometric Mullite,'' *J. Am. Ceram. Soc.*, **68** [1] C-6–C-7 (1985).

[2]T. I. Mah and K. S. Mazdiyasni, ''Mechanical Properties of Mullite,'' *J. Am. Ceram. Soc.*, **66** [10] 699–703 (1983).

[3]K. S. Mazdiyasni and L. M. Brown, ''Synthesis and Mechanical Properties of Stoichiometric Aluminum Silicate (Mullite),'' *J. Am. Ceram. Soc.*, **55** [11] 548–52 (1972).

[4]P. F. Becher, C. H. Hsueh, P. Angelini, and T. N. Tiegs, ''Toughening Behavior in Whisker-Reinforced Ceramic Matrix Composites,'' *J. Am. Ceram. Soc.*, **71** [12] 1050–61 (1988).

[5]P. F. Becher and T. N. Tiegs, ''Toughening Behavior Involving Multiple Mechanisms: Reinforcement and Zirconia Toughening,'' *J. Am. Ceram. Soc.*, **70** [9] 651–54 (1987).

[6]G. C. Wei and P. F. Becher, ''Development of SiC-Whisker-Reinforced Ceramics,'' *Am. Ceram. Soc. Bull.*, **64** [2] 298–304 (1985).

[7]N. Claussen and J. Jahn, ''Mechanical Properties of Sintered, In Situ-Reacted Mullite-Zirconia Composites,'' *J. Am. Ceram. Soc.*, **63** [3–4] 228–29 (1980).

[8]R. Ruh, K. S. Mazdiyasni, and M. G. Mendiratta, ''Mechanical and Microstructural Characterization of Mullite and Mullite–SiC-Whisker and ZrO_2-Toughened-Mullite–SiC-Whisker Composites,'' *J. Am. Ceram. Soc.*, **71** [6] 503–12 (1988).

[9]J. R. Porter and A. H. Chokshi, ''Creep Performance of Silicon Carbide Whisker-Reinforced Alumina,''; pp. 919–28 in *Ceramic Microstructures '86: Role of Interface*. Edited by J. A. Pask and A. G. Evans. Plenum Press, New York, 1987.

[10]M. C. Shaw and K. T. Faber, ''Temperature-Dependence Toughening in Whisker-Reinforced Ceramics''; *ibid*, pp. 929–38.

[11]T. A. Parthasarathy, R. S. Hay, and R. Ruh, ''High-Temperature Deformation of SiC-Whisker-Reinforced MgO-PSZ/Mullite Composites,'' *J. Am. Ceram. Soc.*, **79** [2] 475–83 (1996).

[12]Z. T. Zhang, Y. Huang, L. Zheng, and Z. Z. Jiang, ''Preparation and Mechanical Properties of SiC Whisker and Nanosized Mullite Particulate Reinforced TZP Composites,'' *J. Am. Ceram. Soc.*, **79** [10] 2779–82 (1996).

[13]W. M. Kriven, G. van Tendeloo, T. N. Tiegs, and P. F. Becher, ''Effect of High Temperature Oxidation on the Microstructure and Mechanical Properties of Whisker-Reinforced Ceramics''; see Ref. 9, pp. 939–47.

[14]M. P. Borom, M. K. Brun, and L. E. Szala, ''Kinetics of Oxidation of Carbide and Silicide Dispersed Phases in Oxide Matrices,'' *Adv. Ceram. Mater.*, **3** [5] 491–97 (1988).

[15]H. Y. Liu, K. L. Weisskopf, M. J. Hoffmann, and G. Petzow, ''Oxidation Behavior of SiC Whisker Reinforced Mullite (–ZrO_2) Composites,'' *J. Eur. Ceram. Soc.*, **5,** 123–33 (1989).

[16]K. L. Luthra and H. D. Park, ''Oxidation of Silicon Carbide-Reinforced Oxide-Matrix Composites at 1375° to 1575°C,'' *J. Am. Ceram. Soc.*, **73** [4] 1014–23 (1990).

[17]C. Baudín and J. S. Moya, ''Oxidation of Mullite–Zirconia–Alumina–Silicon Carbide Composites,'' *J. Am. Ceram. Soc.*, **73** [5] 1417–20 (1990).

[18]M. I. Osendi, ''Oxidation Behavior of Mullite–SiC Composites,'' *J. Mater. Sci.*, **25**, 3561–65 (1990).

[19]M. B. Ricoult, ''Oxidation Behavior of SiC-Whisker-Reinforced Alumina–Zirconia Composites,'' *J. Am. Ceram. Soc.*, **74** [8] 1793–802 (1991).

[20]B. W. Sheldon, E. Y. Sun, S. R. Nutt, and J. J. Brennan, ''Oxidation of BN-Coated SiC Fibers in Ceramic Matrix Composites,'' *J. Am. Ceram. Soc.*, **79** [2] 539–43 (1996).

[21]K. N. Lee and R. A. Miller, ''Oxidation Behavior of Mullite-Coated SiC and SiC/SiC Composites under Thermal Cycling between Room Temperature and 1200°–1400°C,'' *J. Am. Ceram. Soc.*, **79** [3] 620–26 (1996).

[22]C. C. Lin, ''Microstructure Development, Phase Stability, and Toughening in Mullite Matrix Composites'' (Chs. 4–6); Ph.D. Thesis. University of Illinois at Urbana–Champaign, Urbana, IL, 1991.

[23]C. C. Lin, A. Zangvil, and R. Ruh, ''Modes of Oxidation in SiC-Reinforced Mullite/ZrO_2-Based Composites: Oxidation vs. Depth Behavior''; unpublished work.

[24]A. Zangvil, Y. Xu, and G. Fu, ''Oxidation Mechanisms of Mullite/ZrO_2/SiC-Platelet Composites''; pp. 1003–14 in Ceramic Transactions, Vol. 46, *Advances in Ceramic-Matrix Composites II*. Edited by J. P. Singh and N. D. Bansal. American Ceramic Society, Westerville, OH, 1994.

[25]C. Y. Tsai, C. C. Lin, A. Zangvil, and A. K. Li, ''Effect of Zirconia Content on the Oxidation Kinetics of Silicon Carbide/Zirconia/Mullite Composites,'' *J. Am. Ceram. Soc.*, **81** [9] 2413–20 (1998).

[26]A. Zangvil, C. C. Lin, and R. Ruh, ''Microstructural Studies in Alkoxide-Derived Mullite/Zirconia/Silicon Carbide-Whisker Composites,'' *J. Am. Ceram. Soc.*, **75** [5] 1254–63 (1992).

[27]K. M. Trappen and R. A. Eppler, ''Reaction of Zirconia with Silica at the Stoichiometry of Zircon,'' *J. Am. Ceram. Soc.*, **72** [6] 882–85 (1989).

[28]L. U. J. T. Ogbuji, ''Effect of Oxide Devitification on Oxidation Kinetics of SiC,'' *J. Am. Ceram. Soc.*, **80** [6] 1544–50 (1997). □